



HAL
open science

Cascade (Dithio)carbonate Ring Opening Reactions for Self-Blowing Polyhydroxythiourethane Foams

Guilhem Coste, Claire Negrell, Sylvain Caillol

► **To cite this version:**

Guilhem Coste, Claire Negrell, Sylvain Caillol. Cascade (Dithio)carbonate Ring Opening Reactions for Self-Blowing Polyhydroxythiourethane Foams. *Macromolecular Rapid Communications*, 2022, Sustainable Green Polymerizations, 43 (13), pp.2100833. 10.1002/marc.202100833 . hal-03715385

HAL Id: hal-03715385

<https://hal.science/hal-03715385>

Submitted on 12 Jul 2022

HAL is a multi-disciplinary open access archive for the deposit and dissemination of scientific research documents, whether they are published or not. The documents may come from teaching and research institutions in France or abroad, or from public or private research centers.

L'archive ouverte pluridisciplinaire **HAL**, est destinée au dépôt et à la diffusion de documents scientifiques de niveau recherche, publiés ou non, émanant des établissements d'enseignement et de recherche français ou étrangers, des laboratoires publics ou privés.

1 Cascade (dithio)carbonate ring opening reactions for self-blowing
2 Polyhydroxythiourethane foams

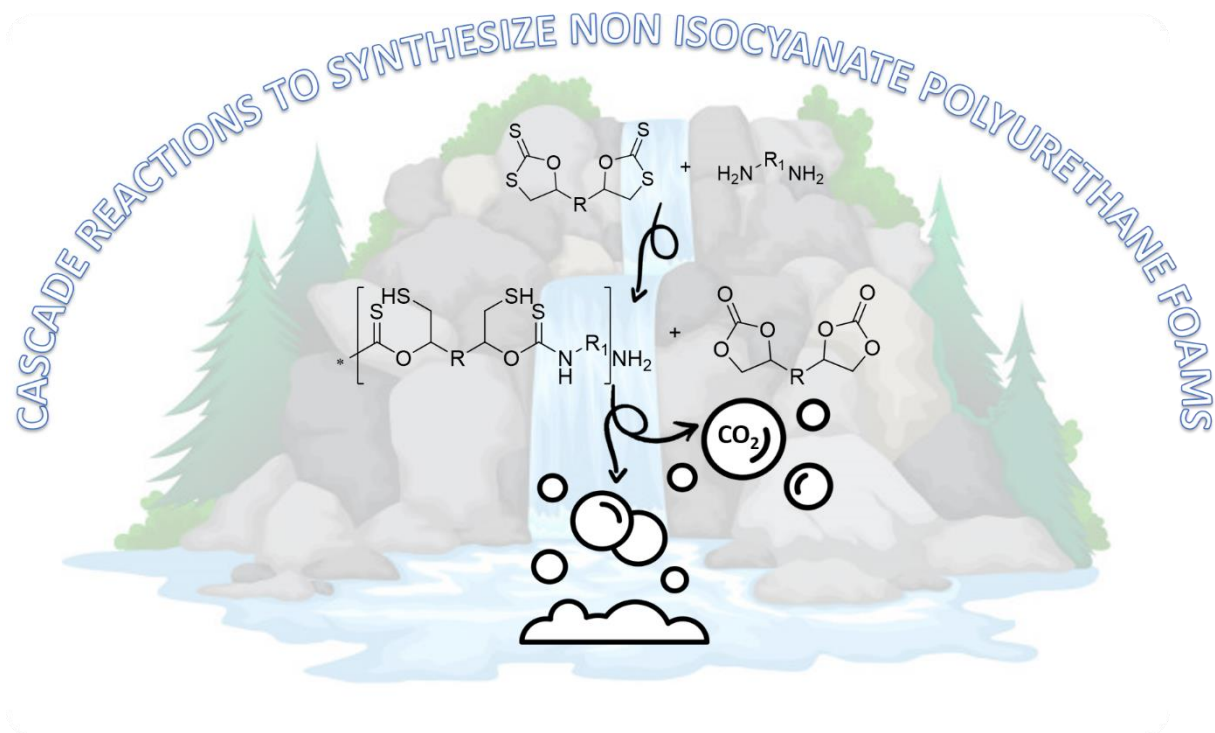
3 Guilhem Coste, Claire Negrell, Sylvain Caillol*

4 ICGM, Univ Montpellier, CNRS, ENSCM, Montpellier, France

5 * Sylvain.caillol@enscm.fr

6 Keywords: Chemical Blowing Agent, Foam, Polyhydroxyurethane, Dithiocarbonate

7



8

9 **Abstract:**

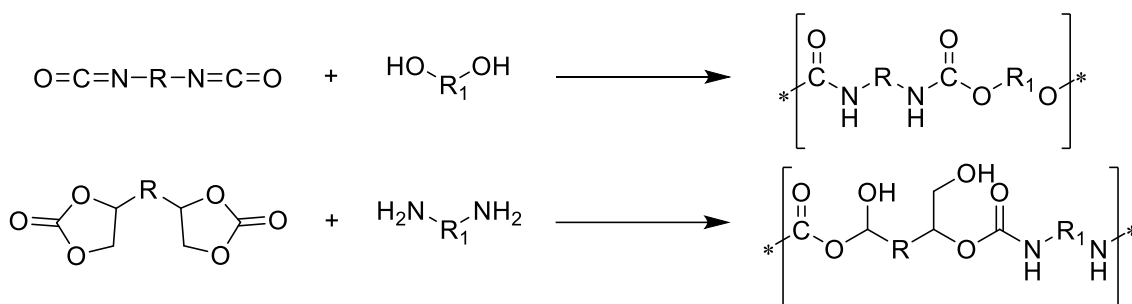
10 Polyurethane (PU) foams are very common materials that have found many applications over the
11 years. Their use is constantly improving due to their unique physical properties and easy blowing which
12 does not require the addition of a blowing agent. Greener routes have been explored in the recent
13 years to replace isocyanates. One of the most promising routes is leading to Polyhydroxyurethanes
14 (PHU). However, with PHUs, external blowing agent are usually required to obtain a foam. Thus, our
15 work focuses on PHU foam synthesis using *in situ* reaction to produce NIPU foam. Hence, the
16 aminolysis of thiocyclic carbonate triggers Pearson reaction between released thiols and cyclic
17 carbonates which serves as a chemical blowing agent.

18 **1. Introduction**

19 Otto Bayer pioneered polyurethanes (PU) during the 30's, derived from the reaction of diisocyanates
20 and polyols.¹ PU have been tailored for multiple applications from wood glue to bed mattresses using
21 the easy variation of the ratio of the two components.^{2,3} Thus, PU are widely used nowadays with more
22 than 20 Mt produced in 2020 particularly for foams applications that represent two thirds of the global

23 production.⁴⁻⁶ The foaming reaction is generally induced by hydrolysis of isocyanates with the release
 24 of carbon dioxide as by-product. The release of gas expands the polymer during the curing, leading to
 25 foams with various properties depending on polyisocyanates and polyols used (scheme 1).⁷ Despite
 26 the importance of PU, the health concerns and regulatory changes associated with the use of toxic
 27 isocyanates such as 4,4'-methylenebis(phenyl isocyanate) or m-tolyldiene diisocyanate have driven
 28 industrial and academic researches to develop isocyanate-free PU foams.^{8,9}

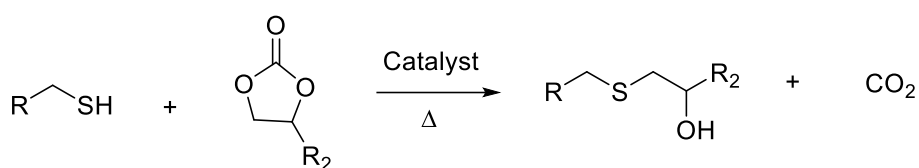
29 In order to design PU without isocyanate, the step-growth copolymerization between amines and 5-
 30 membered cyclic carbonates that leads to non-isocyanate polyurethanes (NIPU) has recently gained
 31 increased attention (scheme 1).¹⁰⁻¹⁵ This is the most promising route to replace the conventional PU
 32 synthesis.¹⁶⁻²⁵ Since a β hydroxy group is created, close to carbamate function, these polymers are
 33 named polyhydroxyurethanes (PHU). Nevertheless, the reaction between cyclocarbonates and amines
 34 does not produce gas unlike isocyanate with water, which limits the use of such promising polymers,
 35 since foams are not easily obtained. In order to overcome this drawback, external blowing agents are
 36 needed to blow the foams. Blattmann *et al.* used a physical blowing agent (PBA) Solkane 365/227
 37 which evaporates during polymer curing and Grignard *et al.* obtained a foam using supercritical
 38 CO₂.^{26,27} Another approach is the utilization of a chemical blowing agent (CBA). Hence, Cornille *et al.*
 39 used this method with a poly(methylhydroxysiloxane) CBA and pioneered the synthesis of PHU foams.
 40 This CBA reacts with amines in order to release H₂ which expands the thermoset during the
 41 polymerization and yields a foam.²⁸ Moreover, this reaction also occurred - slowly - at room
 42 temperature in order to obtain flexible foams.²⁹ Sodium carbonate has also been explored as blowing
 43 agent by Xi *et al.* at 200°C in order to obtain rigid foams.³⁰ More recently, Clark *et al.* used the side
 44 reaction of ring opening of a bis-carbonate at 100°C to produce CO₂ and obtained a foam. However,
 45 this approach remains limited to some monomers whose synthesis is complex which narrows the
 46 interest of this route.^{31,32} In the search for new CBAs, our team recently reported a review dedicated
 47 to current blowing agents including innovative routes to blow foams with new chemical pathways to
 48 produce gases.³³ Recently, Monie *et al.* interestingly prepared for the first time self-blowing PHU foams
 49 using the Pearson reaction *e.g.* the reaction between a nucleophilic thiol and a cyclic carbonate, which
 50 produces CO₂ as co-product (scheme 2). The use of the Pearson reaction is attractive because the
 51 blowing reaction occurs simultaneously with the curing reaction. Moreover the released gas is non-
 52 toxic and non-flammable unlike H₂ or other PBAs.³⁴ However, such reaction requires the use of a thiol
 53 in the formulation with the amine, which could usually confer bad odor. Moreover, the use of volatile
 54 compound could lead to further issues in a formulation, such as leaching or toxicity situations.



55
 56 *Scheme 1: Reactional scheme for PU (top) and PHUs (bottom) synthesis.*

57 Moreover, through the different studies carried out on PHUs, the main drawback remains the low
 58 reactivity of aminolysis of 5-membered cyclic carbonates (5CCs) compare to reaction between alcohol
 59 and isocyanate. In order to overcome this issue, several studies have been conducted. First, more
 60 reactive 5CCs with electron-withdrawing groups have been tested.³⁵⁻³⁷ Then, six-, seven-, eight-
 61 membered or thio-cyclic carbonates have been screened and described as more reactive than usual 5-

62 membered cyclic carbonates.^{35,38,39} However the usual synthesis of six- and higher membered cyclic
 63 carbonates uses triphosgene which limits their interest. A new way of carbonate synthesis has been
 64 developed in order to avoid the use of triphosgene, but the use of such monomer is still limited since
 65 intercarbonation side reaction is possible.⁴⁰⁻⁴² Moreover, different catalysts have been studied in order
 66 to improve the kinetics of aminolysis of cyclic carbonate. Hence, 1,5,7-triazabicyclo [4.4.0]dec-5-ene
 67 and cyclohexylphenyl thiourea have been reported as the best catalysts by Blain *et al.* and Lambeth *et*
 68 *al.*^{43,44} Nevertheless, despite numerous studies carried out in order to improve 5CCs/amine kinetics,
 69 nowadays, only one paper claims the synthesis of a PHU foam at room temperature with a total
 70 conversion.²⁹ Beyond the foam synthesis, some other studies showed a total conversion of PHU with
 71 fast kinetics and catalyst-free.⁴⁵⁻⁴⁷ Additionally, thio-cyclic carbonate or dithiocarbonate (DTC) have
 72 been first synthesized using carbon disulfide instead of CO₂, in one step synthesis, by Endo *et al.*⁴⁸ who
 73 demonstrated their high reactivity. Thus, despite their higher reactivity compare to other cyclic
 74 carbonates, such monomers have still aroused limited interest.^{49,50}

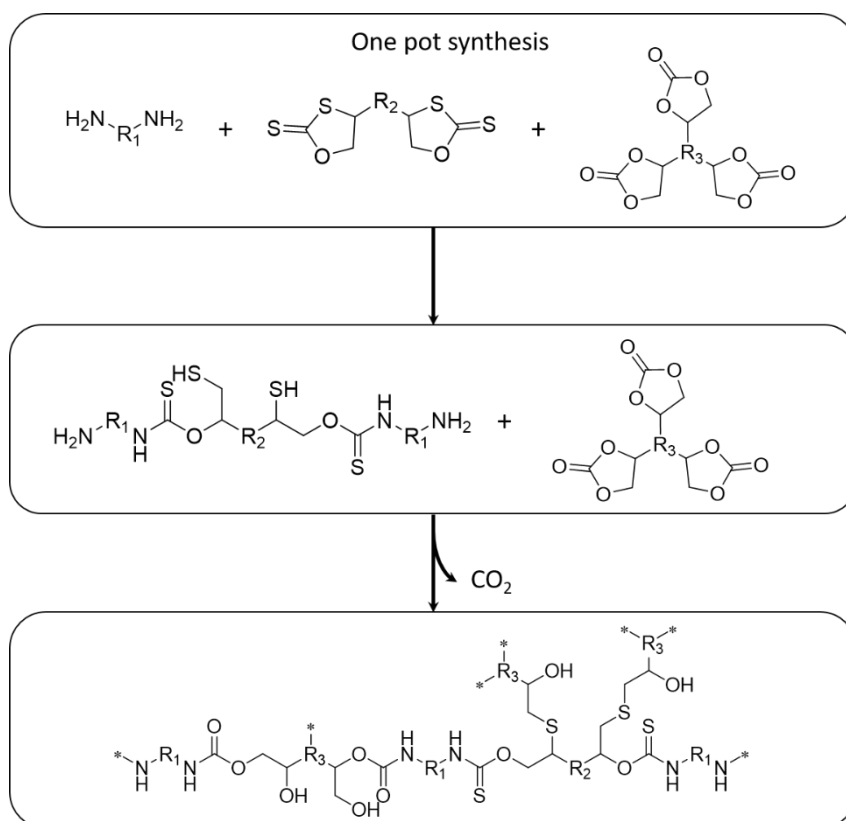


75

76 *Scheme 2: Pearson reaction*

77 In order to increase the reactivity of carbonates and obtain a NIPU foam, a masked thiol could be added
 78 in the polymer matrix.⁵¹ Indeed, thiol moiety is released by the aminolysis of a dithiocarbonate.⁵² We
 79 therefore postulated that combining 5CCs and DTC with amine should lead to two competitive ring-
 80 opening reactions. Hence, on one side could occur the reaction between the amine and DTC, which
 81 leads to β -thiourethanes and CO₂. On the other side is the reaction between the amine and 5CCs, which
 82 leads to hydroxyurethanes. Thus, we hypothesized that a foam could be obtained by mixing amine
 83 with DTC and 5CCs without any external blowing agent.

84 Hence, in the present study, we have chosen to elaborate first self-blowing Non-Isocyanate
 85 PolyThioUrethanes (NIPTUs) foams by the aminolysis of both 5CCs and DTC, which simultaneously
 86 entails a decarboxylation of 5CCs by the thiol formed by DTC/amine reaction. First, difunctional
 87 monomers have been synthesized and characterized. Secondly the foams have been synthesized. At
 88 last, the obtained NIPU foams have been characterized. Moreover, we have proved that CO₂ is the only
 89 gas formed during the curing.



90

91 *Scheme 3: General scheme of the synthesis of PHTU foam*

92

93 2. Experimental section

94 2.1. Materials

95 Poly(propylene glycol) diglycidyl ether ($M_n=640\text{g}\cdot\text{mol}^{-1}$), carbon disulfide (CS_2 , purity 99%),
 96 trimethylolpropane triglycidyl ether, tetrabutylammonium bromide (purity 99%), lithium bromide
 97 (purity 99%), propylene oxide (purity 99%), dodecylamine (purity 99%), 1-dodecanethiol (purity 98%)
 98 were purchased from Sigma-Aldrich (Darmstadt Germany). 1,8-Diazabicyclo [5.4.0]undec-7-ene (DBU)
 99 were purchased from TCI EUROPE N.V (Zwijndrecht, Belgium). Ethyl acetate was purchased from VWR
 100 International S.A.S (Fontenay-sous-Bois, France). Laponite-S 482 was kindly provided by IMCD (Lyon,
 101 France). The TEGOMER E-Si 2330 was provided by Evonik (Amsterdam, Netherlands). The NMR solvent
 102 used is CDCl_3 from Eurisotop.

103 2.2. Characterizations

104 Nuclear Magnetic Resonance

105 Proton Nuclear Magnetic Resonance (^1H NMR) analyses were carried out in deuterated chloroform
 106 (CDCl_3 , 99.50% isotopic purity) using Bruker Avance III 400 MHz NMR spectrometer at a temperature
 107 of 25°C .

108 Fourier Transform Infrared Spectroscopy

109 Infrared (IR) spectra were recorded on a *Nicolet 210 Fourier transform infrared spectroscopy* (FTIR)
 110 spectrometer. The characteristic IR absorptions mentioned in the text where strong bands are
 111 reported in cm^{-1} .

112 Thermogravimetric Analyses

113 Thermogravimetric Analyses (TGA) were carried out using TG 209F1 apparatus (Netzch).
114 Approximately 10 mg of sample were placed in an alumina crucible and heated from room
115 temperature to 800°C at a heating rate of 20 °C/min under nitrogen atmosphere (40 mL/min). A
116 nitrogen flow was used to protect the apparatus.

117 Differential Scanning Calorimetry

118 Differential Scanning Calorimetry (DSC) analyses were carried out using a NETZSCH DSC200F3
119 calorimeter, which was calibrated using indium, n-octadecane and n-octane standards. Nitrogen was
120 used as purge gas. Approximately 10 mg of sample were placed in a perforated aluminum pan and the
121 thermal properties were recorded between -150 °C and 120 °C at 20 °C/min to observe the glass
122 transition temperature. The T_g values were measured on the second heating ramp to erase the
123 thermal history of the polymer. All the reported temperatures are average values on three different
124 tries.

125 Dynamic Mechanical Analyses

126 Dynamic Mechanical Analyses (DMA) were carried out on Metravib DMA 25 with Dynatest 6.8
127 Software. Uniaxial stretching of foam samples (10x15x12 mm³) was performed while heating at a rate
128 of 3°C.min⁻¹ from -120°C to 120°C, keeping frequency at 1Hz.

129 The mechanical compression of the samples was measured at room temperature using 10x15x12 mm³
130 foam samples in the creep mode with compression plate. The static maximum force used was fixed to
131 20 N with application time 60 s and maximum displacement of 30% of strain and the time charging of
132 1 s. Then, the time of recovery of foams was measured during 60 s

133 Hardness

134 Shore 0 hardness for foam was measured on a durometer Shore Hardness Tester HD0 100-1 from
135 Sauter. Samples with 0.5 cm thickness were prepared for the measurement. An average of five
136 measurements was performed.

137 Gel content

138 Three samples from the same material, of around 20 mg each, were separately immersed in THF for
139 24 h. The three samples were then dried in a ventilated oven at 70°C for 24h. The gel content (GC) was
140 calculated using equation (5), where m₂ is the mass of the dried material and m₁ is the initial mass.
141 Reported gel content are average values of the three samples.

$$GC = \frac{m_2}{m_1} \times 100 \quad (4)$$

142 Scanning electron microscopy

143 The morphology and the internal structure of the foams were analyzed using in parallel surface to the
144 rise direction of NIPU foam by scanning electron microscopy (SEM). A FEI Quanta 200 FEG was used to
145 obtained foam images.

146 Optic microscopy

147 Due to the pores size few foams were analyzed by optic microscopy. A Leica DM 6000 M was used.

148 Rheological experiments

149 The gelation times were measured using a Thermo Fisher HAAKE MARS rheometer with a plate– plate
150 geometry with a diameter of 25 mm. The gelation times were analyzed by observing the crossover of
151 the storage modulus (G) and loss modulus (G) during an oscillatory experiment at 1 Hz, 90 °C and 2%
152 of deformation, according to the previously determined linear domain.

153 Titration of the amine equivalent weight of Jeffamine EDR-148 by ¹H NMR

154 The Amine Equivalent Weight (AEW) is the amount of product needed for one equivalent of reactive
155 amine function. It was determined by ¹H NMR using and internal standard (benzophenone). A known
156 mass of product and benzophenone were poured into an NMR tube and 550 μL of CDCl₃.were added.
157 The AEW was determined using equation (5) by comparing the integration value of the signals assigned
158 to the benzophenone protons (7.5-7.8 ppm) with the integration of the signals arising from amine
159 moiety protons (2.67 ppm).

$$AEW = \frac{\int PhCOPh \times H_{amine}}{\int amine \times H_{PhOCPh}} \times \frac{m_{amine}}{m_{PhOCPh}} \times M_{PhCOPh} \quad (5)$$

160 \int_{PhCOPh} : integration of the signal from benzophenone protons; \int_{amine} : integration of the signals from
161 protons in α the amine function; H_{amine} : number of protons in α of the amine function; H_{PhOCPh} : number
162 of benzophenone protons; m_{amine} : amine mass; m_{PhOCPh} : benzophenone mass; M_{PhCOPh} : benzophenone
163 molecular weight.

164 Titration of the carbonate equivalent weight by ¹H NMR

165 The Carbonate Equivalent Weight (CEW) is the amount of product needed for one equivalent of
166 reactive cyclic carbonate or thiocarbonate function. It was determined by ¹H NMR using and internal
167 standard (benzophenone). A known mass of product and benzophenone were poured into an NMR
168 tube and 550 μL of CDCl₃.were added. The CEW was determined using equation (6) by comparing the
169 integration value of the signals assigned to the benzophenone protons (7.5-7.8 ppm) with the
170 integration of the signals arising from cyclic carbonate (4.85 ppm for TMPTC and 5.25 ppm for
171 polypropylene oxide bis-thiocarbonate).

$$CEW = \frac{\int PhCOPh \times H_{carbonate}}{\int carbonate \times H_{PhOCPh}} \times \frac{m_{carbonate}}{m_{PhOCPh}} \times M_{PhCOPh} \quad (6)$$

172 \int_{PhCOPh} : integration of the signal from benzophenone protons; $\int_{carbonate}$: integration of the signals from
173 protons in α the carbonate function; $H_{carbonate}$: number of protons in α of the carbonate function;
174 H_{PhOCPh} : number of benzophenone protons; $m_{carbonate}$: product mass; m_{PhOCPh} : benzophenone mass;
175 M_{PhCOPh} : benzophenone molecular weight.

176 2.3. Synthesis

177 Monomer synthesis

178 Synthesis of trimethylpropane tricarboxylate (TMPTC)

179 Trimethylolpropane triglycidyl ether (TMPTGE; 300 g, 0.99 mol) and tetrabutylammonium bromide
180 (TBAB; 9.596 g, 0.029 mmol) were solubilized in 100 mL of AcOEt and added to a 600 mL sealed reactor.
181 The reaction was carried out at 80 °C under 20 bars of CO₂ for 120 h. The crude mixture was then
182 washed with water and brine to remove TBAB. The organic layer was then dried with magnesium
183 sulfate and under vacuum. The pure product was obtained as a yellowish viscous liquid (yield = 90%).

184 ¹H NMR (400 MHz, CDCl₃): δ /ppm = 0.84 (t, CH₃), 1.41 (m, CH₂), 3.28-4.03 (m, CH₂), 4.46 (m, CH₂), 4.49
185 (t, CH₂), 4.85 (m, CH).

186 Synthesis of polypropylene oxide bis-thiocarbonate (PPOTC)

187 Poly(propylene oxide) diglycidyl ether $\overline{M}_n = 640$ g.mol⁻¹ (PPO-GE-640) and LiBr (0.55 g, 0.0063 mmol)
188 were solubilized in 100 mL of EtOAc and added in a two-necked round bottom flask equipped with a
189 condenser. The mixture was heated at 60°C and then CS₂ (47.58 g, 0.625 mol) was added. The reaction
190 was carried out 96 hours at 60°C. The CS₂ was then evaporated and the crude mixture was then washed
191 with water and brine to remove LiBr. The organic layer was then dried with magnesium sulfate and
192 under vacuum. The pure product was obtained as a viscous yellowish liquid (yield= 85%)

193 ¹H NMR (400 MHz, CDCl₃): δ/ppm = 1.16 (m, CH₃), 3.32-4.1 (m, CH₂, CH), 5.25 (m, CH)

194 General procedure of foam synthesis

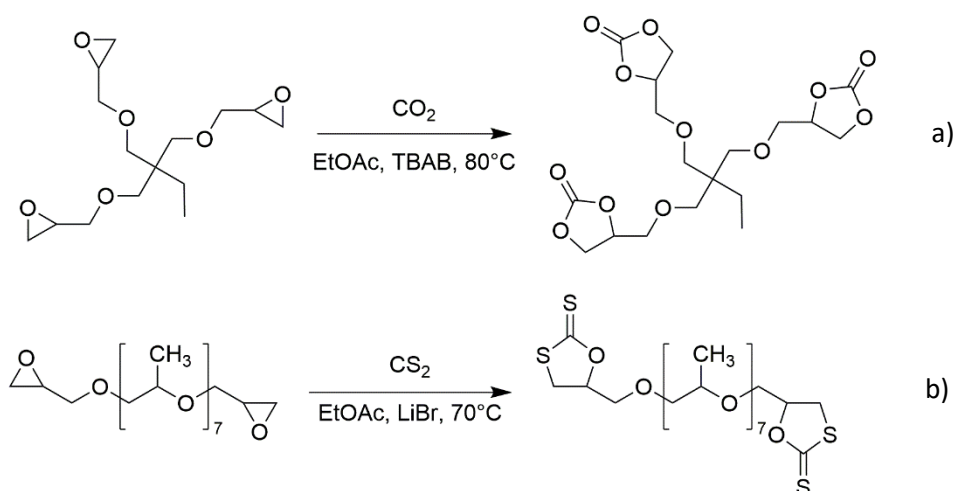
195 Materials were synthesized with a cyclic carbonate or PPOTC molar/amine ratio of 1/1. The amine and
196 carbonate masses were calculated with the equation (6) and (7), respectively, where n_{carbonate} and n_{amine}
197 are the number of moles of cyclic carbonate amine, and AEW is the amine equivalent weight and CEW
198 is the carbonate equivalent weight. The formulations of NIPTUs foams were calculated from 1
199 equivalent of carbonate, 1 equivalent of amine, 0.05 molar equivalent of DBU in relation to the
200 carbonate. The mass targeted for each formulation is approximately 10g. First, the TMPTC and DBU
201 were placed in the silicone mold and mixed manually 2 minutes. Then the PPOTC was added to the
202 mixture and stirred 2 more minutes. Finally, the EDR-148 was poured and the mixture was, once again,
203 stirred 2 minutes. The obtained foamed mixture was heated at 90°C for 24h. All additives were used
204 following the technical data sheet of the suppliers

205 3. Results & Discussion

206 Synthesis and characterizations of raw materials

207 Before the synthesis of the monomers and the NIPTUs foams, a complete characterization of raw
208 materials has been carried out to determine the functionality of trimethylolpropane tricarboxylate and
209 polypropylene oxide bis-thiocarbonate. Moreover, the NH₂ functionality of the 2,2'-
210 (ethylenedioxy)bis(ethylamine) EDR-148 was calculated.

211 The trimethylolpropane tricarboxylate (TMPTC) was synthesized by carbonation reaction of commercial
212 trimethylolpropane triglycidyl ether in presence of tetrabutylammonium bromide and EtOAc (Scheme
213 4a). Polypropylene oxide bis-thiocarbonate (PPOTC) was synthesized by thiocarbonation reaction of
214 commercial poly(propylene oxide) diglycidyl ether (PPO-DE, $\overline{M}_n = 640$ g.mol⁻¹) in presence of lithium
215 bromide and EtOAc (Scheme 4b). Their structures have been confirmed by ¹H NMR (Figures S3 and S4).
216 In order to establish exactly the carbonate functionality (CEW) of cyclic carbonate and cyclic
217 thiocarbonate, ¹H NMR analyses with standard solution (CDCl₃ with 10-20mg of Benzophenone) were
218 achieved. The CEW presented in Table 1 is the average of three different titrations. The obtained CEW
219 of the TMPTC is below 3, this result is not linked to uncompleted conversion of the epoxide during the
220 carbonation reaction. It is linked to the uncompleted epoxidation of the trimethylolpropane with
221 epichlorohydrin since the TMPTGE received has a functionality of 2.6.



222 Scheme 4: a) Carbonation of TMPTC b) Thiocarbonation of PPO-DE

223 Amine

224 In order to obtain the alternative NIPUs foams, the Jeffamine EDR-148 (EDR 148) was tested with both
 225 TMPTC and PPOTC. The ^1H NMR spectrum of the EDR-148 confirms the di-functionality of this amine
 226 (Figure S5). Actually, the peak of the amine function (NH_2) at 0.8 ppm integrates for 3.87 protons.
 227 Indeed, EDR 148 is based on ethylene glycol and contains two primary amine groups with an oxygen
 228 in γ position relative to amine group inducing high reactivity of the amine.

Reactants	CEW ($\text{g}\cdot\text{eq}^{-1}$)	AHEW ($\text{g}\cdot\text{eq}^{-1}$)	Carbonate, thiocarbonate or amine functions	\bar{M} ($\text{g}\cdot\text{mol}^{-1}$)
TMPTC	184	-	2.6	476
PPOTC	440	-	1.8	792
EDR-148	-	74	2	148

229 Table 1: Characterization of reactants. CEW= average of three ^1H NMR, AHEW calculated by ^1H NMR.

230 Foam preparation

231 In this study, four foams have been prepared at 90°C from TMPTC and PPOTC in combination with EDR-
 232 148. The TMPTC has a functionality of 2.6 (Table 1), therefore, this compound could confer rigidity to
 233 the system through the crosslinking with the diamine. 1,8-Diazabicyclo[5.4.0]undec-7-ene (DBU) has
 234 been identified as the best catalyst by Monie *et al.* to catalyze the reaction between thiol and
 235 cyclocarbonate.³⁴ No blowing agent is added since the aim of this work is to use the reaction of the *in*
 236 *situ* produced thiol with cyclic carbonate in order to produce CO_2 . A ratio 1:1 of amine:cyclic
 237 carbonate/DTC is used during this study. Nevertheless, these formulations do not take into account
 238 the reaction between thiol and cyclic carbonate. A slight default of amine should be used since cyclic
 239 carbonates react with the thiol. Thus, an optimization of the formulation has been carried out to
 240 determine the best ratio amine:cyclic carbonate/DTC. The highest T_g was obtained for the
 241 stoichiometry 1:1 (amine:carbonate), the result are presented in supporting information (Figure S7).
 242 These foams were prepared following the formulation based on carbonate equivalent weight (CEW)
 243 and amine reactive hydrogen equivalent weight (AHEW) from Table 2. First, we added the TMPTC, DBU
 244 and dithiocarbonate. The mixture was mixed manually 2 min then the amine was added and mixed
 245 two more minutes. Then, the formulations were poured in a silicone mold and heated at 90°C during
 246 24h. To improve the shape of the foam, Laponite S482 (Laponite) additive was used.⁵³ This
 247 additive acts as a nucleating agent by the stabilization of the cells. Homogeneous foam with small cells

248 are expected with Laponite S482. Additionally, the TEGOMER E-Si 2330 (Tegomer) was added. This
 249 polydimethylsiloxane containing unreactive epoxy acts as a surfacing agent.

250 The differences of structure of NIPU foams were observed by scanning electron microscopy (SEM) or
 251 optic microscopy. Moreover, the measurement of the apparent density and dynamic mechanical
 252 analysis (DMA) completed the analyses of foam structure. Then, the cross-linking degree was
 253 determined by measurement of the swelling and insoluble contents. Finally, thermal and thermo-
 254 mechanical properties of NIPU foams were characterized by differential scanning calorimetry (DSC),
 255 thermogravimetric analysis (TGA) and dynamic mechanical analysis (DMA).

Foam	Equivalents				Additive (5wt%)
	TMPTC	PPOTC	EDR148	DBU	
1	0.7	0.3	1	0	-
2	0.7	0.3	1	0.03	-
3	0.7	0.3	1	0.03	Tegomer
4	0.7	0.3	1	0.03	Laponite

256

257 *Table 2: NIPU foam formulations in equivalent.*

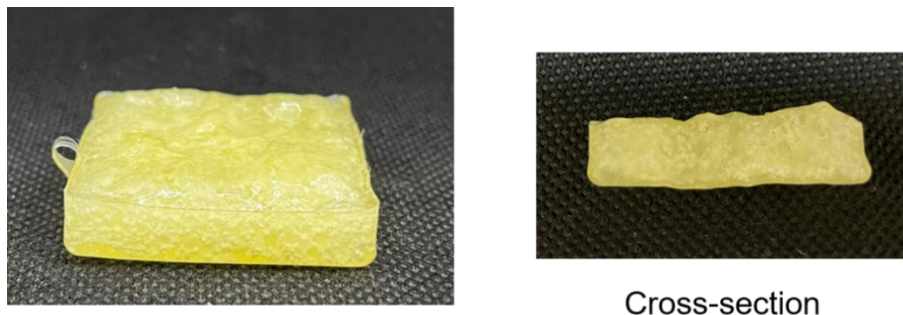
258 Structural characterization of NIPU foams

259 First, the foams were characterized visually in order to compare the homogeneity according to the
 260 formulation. From this first characterization, it can be concluded that there is a need to use a catalyst
 261 since the foam 1 (Table 2) collapsed during baking to give a thermosetting material without any cell.
 262 Such result could be explained by a longer period to obtain the adequate viscosity to maintain the gas
 263 in the material. Tests were carried out in order to define which ratio TMPTC / PPOTC is necessary to
 264 obtain a foam. Indeed, TMPTC is trifunctional and allows crosslinking and PPOTC flexibility between
 265 cross-linking nodes. Thus the ratio between the two monomer is important to have a foam with a great
 266 shape. The results presented in Table 3 show a ratio minimum of TMPTC about 0.7 equivalent. Indeed,
 267 when the TMPTC has a lower ratio the foam collapsed. Thus, 0.7 equivalent defined the limit of TMPTC
 268 to use in order to obtain a foam. For the following experiments the ratio was kept as 0.7 TMPTC and
 269 0.3 PPOTC. Hence, the higher could be the ratio of PPOTC, the more CO₂ we could produce. Then, the
 270 ratio amine:cyclocarbonate/DTC was optimized. The material with highest T_g corresponds to the best
 271 ratio. It was obtained for a ratio 1:1. Hence, the reaction between the thiol and the cyclic carbonate
 272 does not modify the theoretical ratio.

Equivalent of TMPTC	Equivalent of PPOTC	Result
0.5	0.5	No foam
0.6	0.4	No foam
0.7	0.3	Foam

273 *Table 3: Determination of the ratio TMPTC/PPOTC for further experiment. Result observed after 24h at 90°C.*

274 Thereafter, since our system is more reactive than the system using 5CCs, foams synthesis was carried
275 out at 50°C. A porous material has been obtained with little cells (0.30 ± 0.02 mm) and with a high
276 density (0.843 g.cm⁻³). The figure 1 shows the porous material obtained at 50°C.

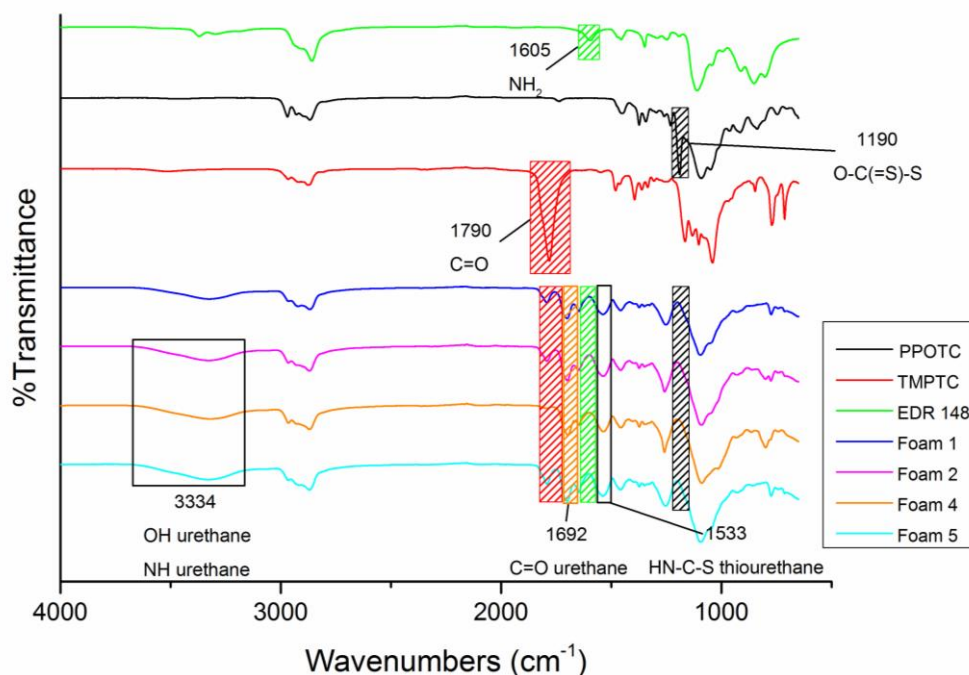


277 *Figure 1: Picture of the NIPU foam obtain at 50°C.*

278 In order to obtain a foam with a higher expansion and a better shape, the following foam were carried
279 out at 90°C. These foams were cured at 90°C during 24 hours. Infrared spectroscopy analysis was
280 performed to check the complete conversion of carbonate and thiocarbonate groups respectively from
281 TMPTC and PPOTC with EDR 148. The FTIR analysis of the foam confirmed the conversion of the
282 dithiocarbonate with the disappearance of the C=S band around 1190 cm⁻¹ of the PPOTC (Figure 2).
283 According to the C=S band disappearance, the appearance of the characteristic band of thiourethane
284 elongation N-C(=S)-O was observed at 1533 cm⁻¹.⁵⁰ Moreover, we observed the disappearance of the
285 bands characteristic of the carbonate groups C=O bond stretching at 1790 cm⁻¹. The appearance of the
286 characteristic band at 1692 cm⁻¹ corresponding to elongation of urethane C=O bond confirmed the
287 conversion of the cyclic carbonate. Finally, the characteristic bands of the N-H amine of the urethane
288 and the hydroxy groups due to the ring opening of the carbonate appeared respectively as wide peaks
289 between at 3150 cm⁻¹ and 3615 cm⁻¹. These results prove the total conversion of the thiocarbonate
290 and the formation of the thiourethane bond. The thiol formed *in situ* during the foam synthesis is also
291 totally consumed since the S-H characteristic band at 2600 cm⁻¹ is not present after 24h at 90°C.

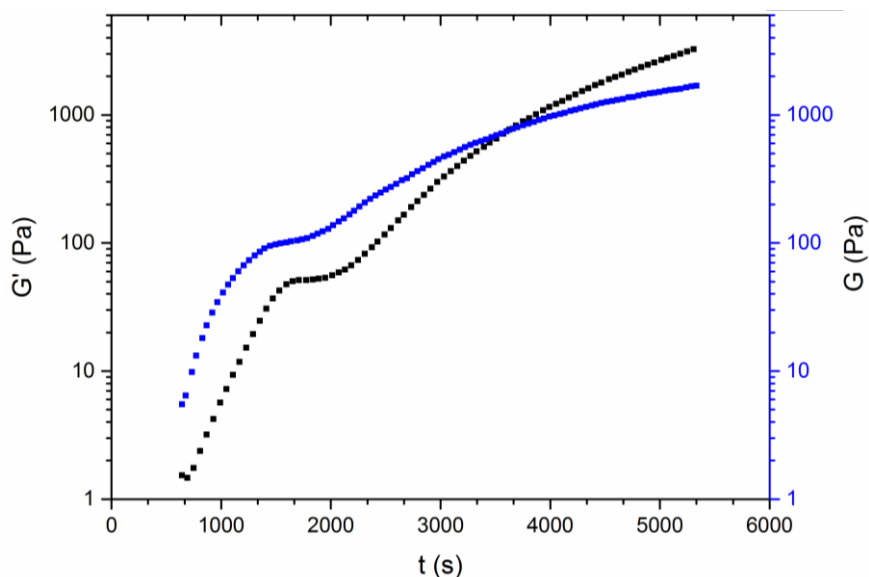
292 Nevertheless, FTIR analysis showed a peak at 1790 cm⁻¹ corresponding to C=O elongation of the cyclic
293 carbonate after the curing. It means that the conversion of the cyclic carbonate functions is not
294 complete. Despite optimized stoichiometry and extended curing at 120°C during 2h, the cyclic
295 carbonate peak is still present in FTIR spectra (figure S12 and S14). The remaining functions are blocked
296 in the cured material. Such result is coherent with the different results obtained by other researchers
297 whom obtained conversion around 80%.^{54,55}

298 In addition, a rheology experiment was carried out in order to determine the gel time of additive-free
299 formulation (figure 3). At 90°C the gel time is obtained in 3700 seconds, approximatively one hour. The
300 rheological experiments gave information on the kinetics of reaction too. Indeed, the viscosity of the
301 formulation rapidly increased to reach a plateau. The quick increase of the viscosity is due to the
302 reaction between the amine and the dithiocarbonate. Then the curing of the TMPTC leads to the gel
303 point.



304 *Figure 2: IR analysis of the reactants and the different NIPU foams after 24h at 90°C.*

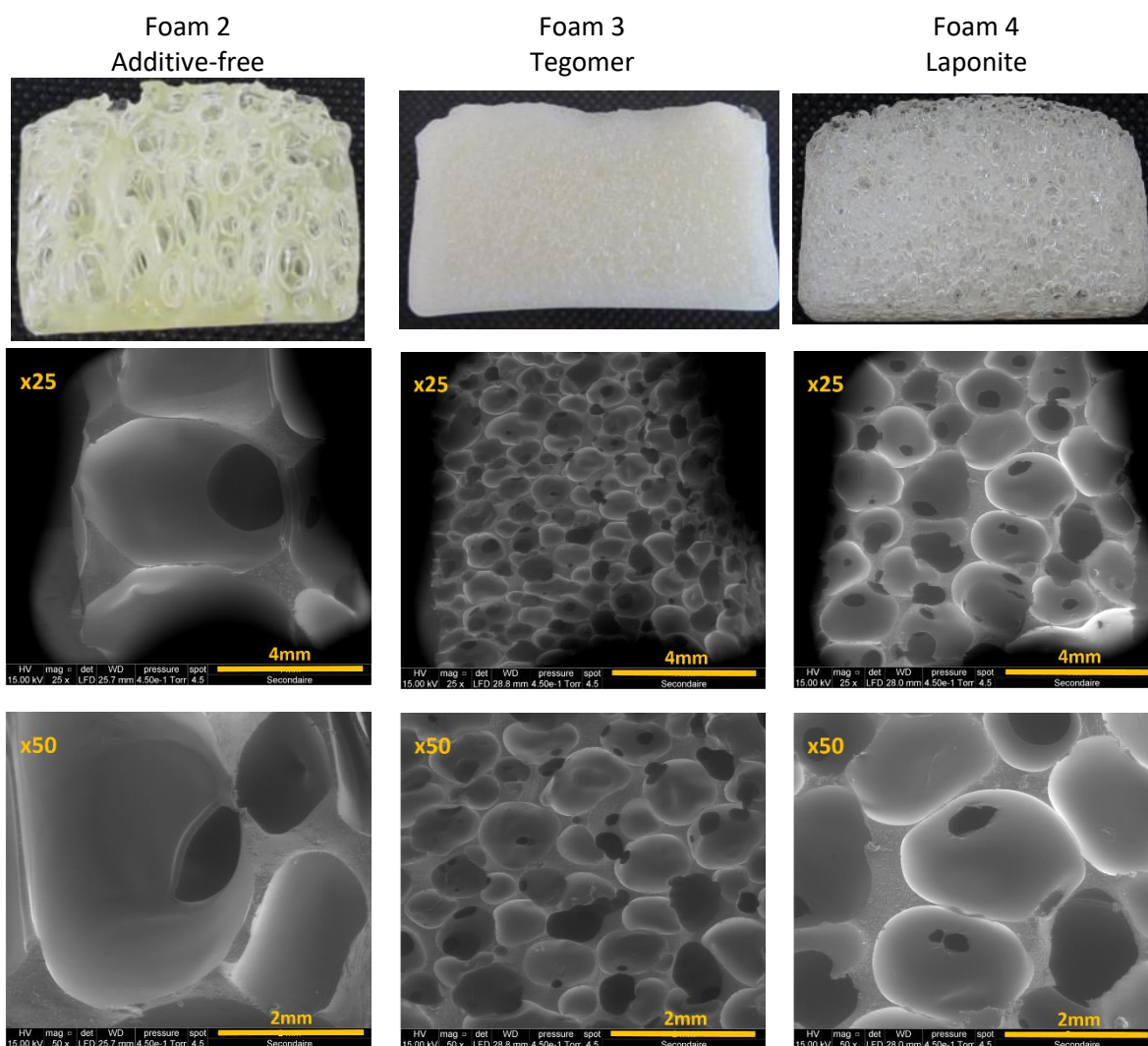
305 Gel content (GC) measurements have been carried out. For all foams, the GC obtained are about 85%
 306 (table 4). These results confirmed the presence of a cured network. The residual cyclic carbonate
 307 functions could explain the non-quantitative gel content.



308 *Figure 3: Gel point analysis of the formulation 2 at 90°C.*

309 After the preliminary experiments, the formulations have been synthesized. First, the foam 2 showed
 310 a relative homogeneity. Indeed, the pores exhibit similar sizes but the pore are not well-distributed in
 311 the foam (figure 4). The foam showed cells with a size 3.8 ± 1.1 mm (table 4). Wide cells are obtained
 312 during the synthesis of foam 2. It is linked to the non-stabilization of the cells during their formation
 313 leading to the cells coalescence. To improve the stabilization of the cells, two additives were added
 314 and led to homogeneous foams, foam 3 and 4 (figure 4). The use of the additives led to the
 315 improvement of the cells number, which corresponds to the stabilization of cells. The effect of each
 316 additive has been explained in the literature by Peyrton *et al.*⁵⁶ Foams 3 and 4 exhibit higher
 317 homogeneity, with higher number of cells and with same, reduced sizes, which confirms the effect of

318 the additives (Table 4). The apparent density (ρ_a) of the foams varies between 0.249 to 0.445 g.cm⁻³.
 319 These foams are characterized as high-density foams since usual PU foams have density around 0.02
 320 g.cm⁻³. The ration A_h/A_c showed an important decrease when additives are used. It shows the effect of
 321 both additives on the foam structure. Indeed, without additives the foams have a structure with a lot
 322 of interconnected cells and the use of additives allows to improve the number of closed cells.
 323 Nevertheless, the difference between the Tegomer and the Laponite is low. So, no conclusion on the
 324 best additive is possible. The results obtained is this part are in adequation with the work carried out
 325 by Monie *et al.* on PHUs foam using these two additives.³⁴



326 Figure 4: SEM pictures of NIPU foams

327

Foam	Cell size (mm)	ρ_a (g.cm ⁻³)	Cell density (Ncell) (cells.cm ⁻³)	A_h/A_c	Gel Content (%)
2	3.8±1.1	0.364	175±3	0.422	83
3	0.79±0.3	0.445	80000±250	0.132	83
4	1.06±0.5	0.249	23000±110	0.152	82

328 Table 4: Main physical characteristic values of the NIPUs foams.

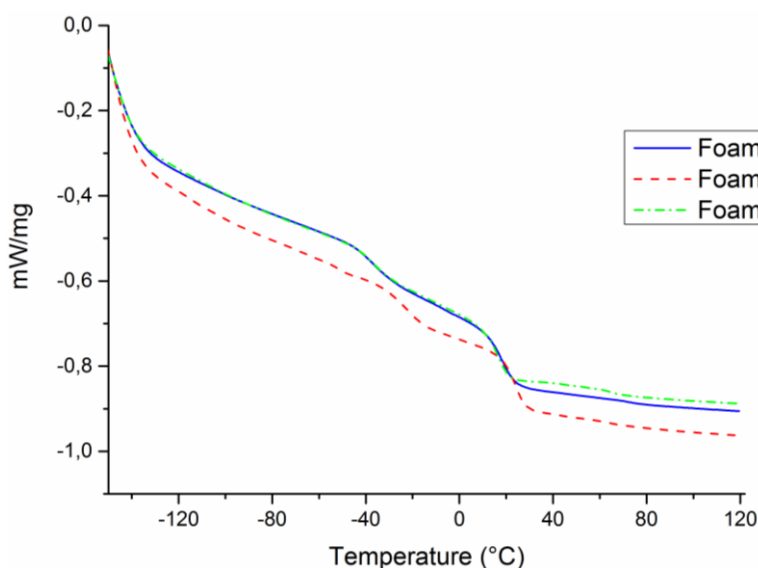
329 Thermal characterization

330 First, thermal properties were measured by differential scanning calorimetry (DSC). Two dynamic
 331 ramps were performed between -100°C and +100°C at 20°C.min⁻¹ under nitrogen flow. Results of DSC
 332 measurements are shown in Table 5. The foams presented two T_g which means that the polymer has
 333 two phases. The first one corresponds to the phase rich in PPOTC and the second one corresponds to
 334 the phase rich in cross-linked TMPTC. This result is supported by the work of Besse *et al.*, Cornille *et al.*
 335 and Tomita *et al.* who demonstrated the higher reactivity of thiocarbonates compared to regular
 336 cyclocarbonates.^{35,52,57} Moreover, our group synthesized PHU foams using the same formulations
 337 replacing the DTC monomer by a difunctional cyclocarbonate and only one T_g is observed.⁵⁸ The PPOTC
 338 leads to lower T_g than the TMPTC. Moreover, the difference of ΔCp of each glass transition on the DSC
 339 thermogram (figure 5) shows a substantial difference between the two T_g which can be linked to the
 340 amount of monomer introduced in the formulation. All the T_g follow the same trend which is consistent
 341 with the formulation since their only difference is the additive used. Moreover, the additives have
 342 been chosen to improve the foam shape and not their thermal properties. Nevertheless, the use of
 343 silica in the Tegomer might improve the thermal degradability since the silica is stable at 800°C.

Foams	T _{d5%}	T _{g1} (°C)	T _{g2} (°C)	Stress (kPa)	Recovery t (s)	Shore Hardness
2	231	-45	12	66	0.52	2.94 ± 1.45
3	245	-31	19	135	12.59	5.74 ± 1.26
4	235	-44	11	57	13.61	1.38 ± 0.44

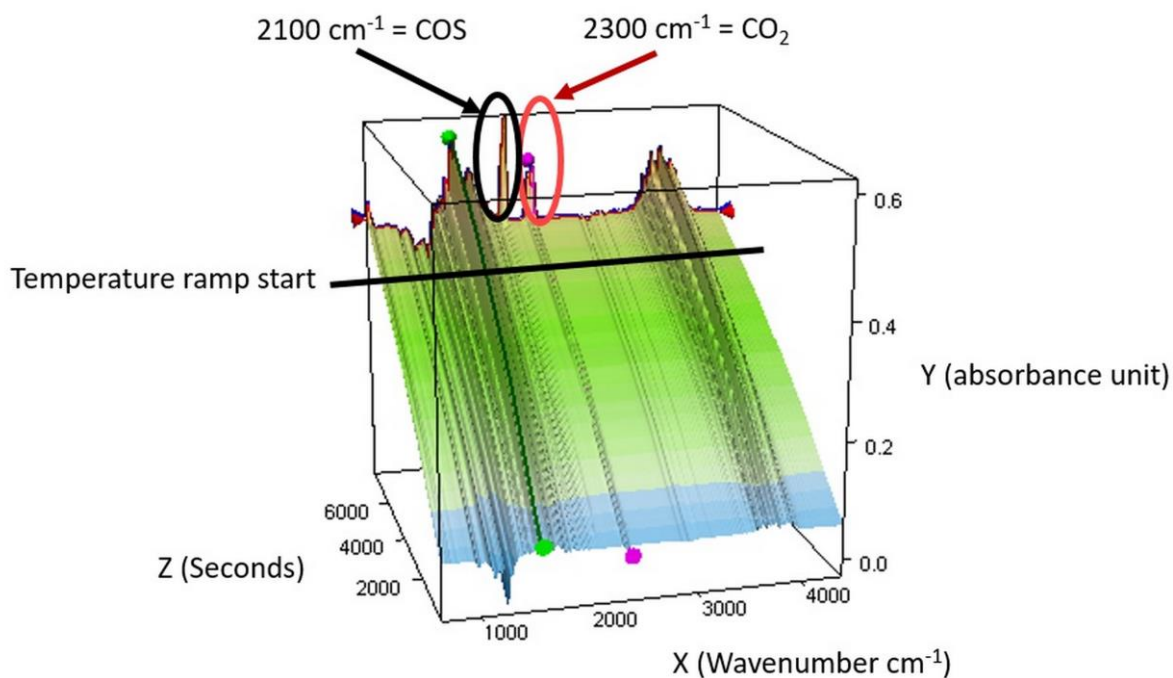
344 Table 5: Thermomechanical properties of the NIPU foams

345 Thermal stability of the foams was also determined using thermogravimetric analysis (TGA) under inert
 346 gas (nitrogen). The results are presented in Figure S19. The thermal degradation temperatures (T_{d5%})
 347 are around 230°C for all foams. However, the foam containing Tegomer presented a higher amount of
 348 residue at 800°C since it contains silica, which is stable at 800°C (Figure S19). The foam 4 presented
 349 also a similar amount of residue due to the presence of clay, which remained undecomposed at 800°C
 350 (figure S19).



351
 352 Figure 5: DSC thermograms of the NIPUs foam. 2nde dynamic ramp after an isotherm of 1h at 120°C.

353 Another thermal analysis was carried out to determine the production of COS and other sulfuric
354 containing gases during the curing. A formulation of similar to the foam 2 was prepared and then a
355 sample between 30-40mg was introduced in a TGA equipped with an FTIR gas detector. The
356 formulation without additive was then heated at 90°C during 2h followed by a temperature ramp to
357 200°C at 20°C/min. The figure 6 shows the 3D IR spectra. On figure 6, we observe that CO₂ is produced
358 during all the curing since a characteristic peak is detected at 2300 cm⁻¹. Thus, COS is not detected
359 during the curing. Nevertheless, during thermal decomposition a characteristic peak of sulfuric gases
360 is detected at 2100 cm⁻¹. Usually sulfuric compound can be decomposed in different gases such as SO₂
361 if there is oxygen nearby the sulfur.⁵⁹ Some other sulfuric compound can be produced during the
362 thermal decomposition of a polymer containing sulfur such as COS or SH₂. Depending on the result
363 obtained in IR analysis (Figure 6) COS is detected during decomposition.⁶⁰ The material seems to
364 release gases containing sulfur at higher temperature but the thermal properties can be improved
365 using flame retardant additives for example, since the sulfur is envisaged as possible candidate for
366 flame retardant synergistic additives.



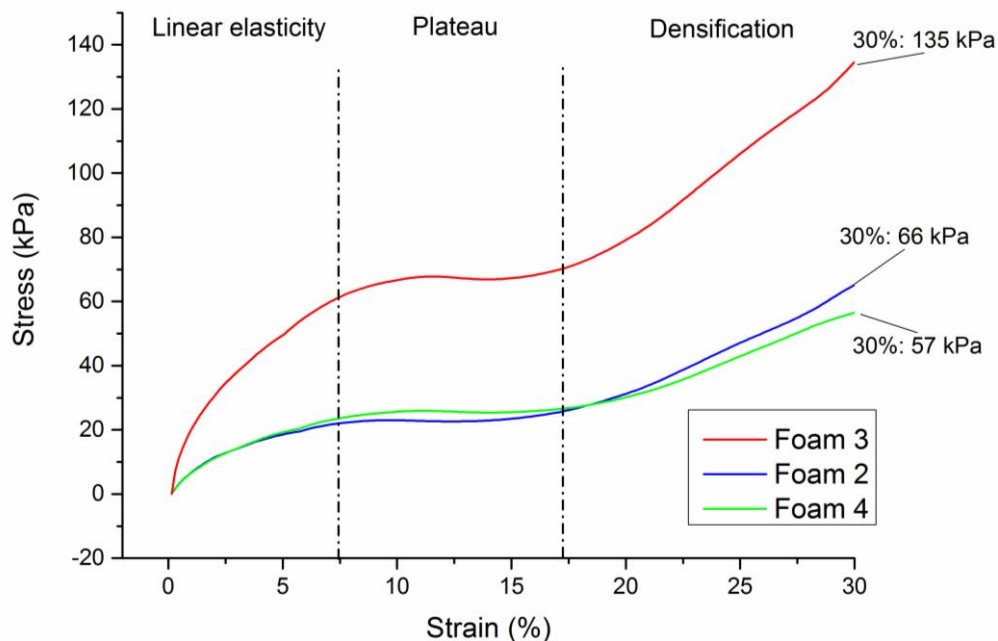
367

368 *Figure 6: IR 3D spectrum of the formulation cured at 90°C during 2 hours and then a ramp to 200°C (red line).*

369

370 Mechanical analysis

371 Dynamic mechanical characterization of NIPU foams was carried out. In order to analyze these
372 samples, two tests were performed. The first test corresponds to the study of the behavior of foams
373 subjected to a stress in monotonic tension (Figure 7). The second test focuses on the recovery time of
374 the foam after a compression at 30% of strain in parallel direction to the foam growth direction (Figure
375 7). The last analysis corresponds to the hardness study of each sample using a Shore 0 test, designed
376 for foams. Before analysis the foam samples were cut in cuboid shapes with an average size of 10 x 12
377 x 13 mm. Afterward, the samples were analyzed with compression plate.

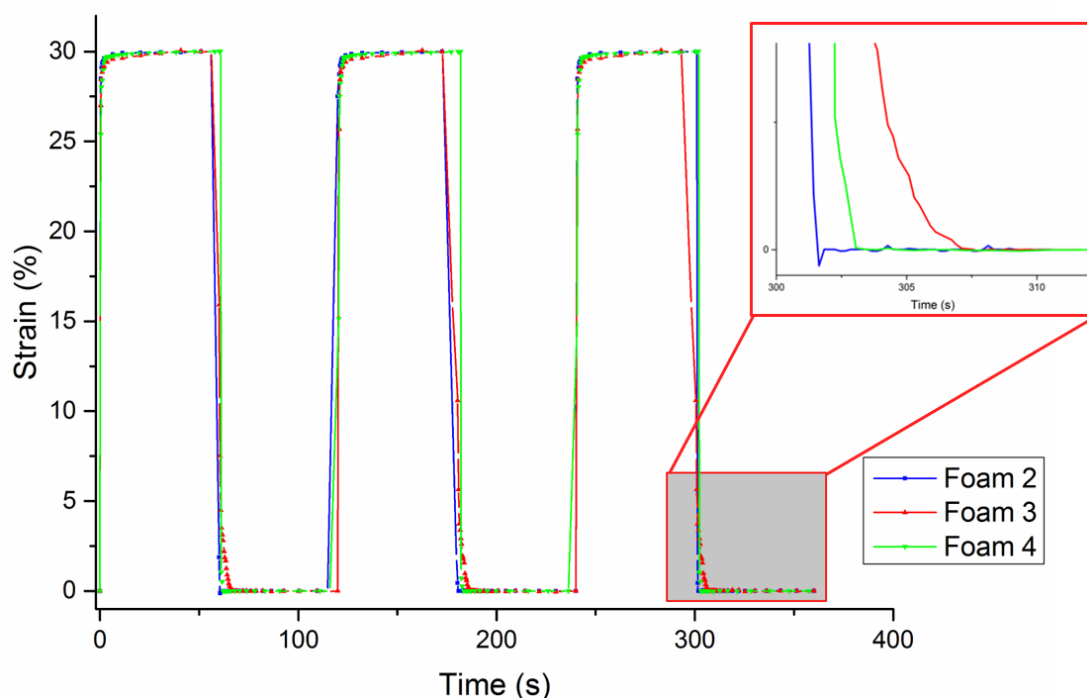


378 *Figure 7: DMA analysis in monotonic tension at room temperature.*

379 The experiment in monotonic compression shows different behaviors. In fact, each of the three foams
380 presented in Figure 7 shows the same three regions. Each of these regions corresponds to different
381 steps. The first region corresponds to the linear elasticity and is equivalent to the strain for edge
382 bending of the foam. The second region, a plateau, corresponds to the collapse of the foam induced
383 by the compression of the cells. Finally, the third region is easily observed by a substantial increasing
384 of the stress for a lower strain. This region corresponds to the densification of the materials when all
385 the cells are entirely compressed. In the Figure 7, all the materials exhibit these three regions. Thus,
386 for the foam 2 and 4 with big cells, the linear elasticity regions are smaller than for foam 3. Such result
387 is explained by the presence of interconnected big cells, which reduces the linear elasticity but
388 increases the plateau region. Accordingly, with the results in table 5, the higher is the density of the
389 foam, the higher is the stress to be applied to compress the foam. Thus, foam 3 exhibits higher stress
390 than foams 2 and 4.

391 The second experiment explores the recovery of foams to the initial state. Hence, the materials were
392 compressed 3 times 60 seconds at 30% of strain and the time of recovery was recorded (Figure 8).
393 From this graphic, all the tested samples recovered 99% of their initial shape in less than 30 seconds.
394 The structure of the foam does not affect significantly the recovery time after three compressions. The
395 foam 3 needed a longer recovery time for all the three compressions. The longer recovery time of the
396 foam 3 is due to the rigidity of the foam, which leads to longer time to recover the final shape. The
397 results of the compression experiment are summarized in the table 5. The third and last experiment
398 determines the hardness of each sample. The data recorded are summarized in Table 5. The results of

399 the hardness experiments confirmed the results obtained with the recovery time experiment and the
400 monotonic tension. Indeed, the foam 4 has the lowest hardness value and the foam 3 has the highest.



401 *Figure 8: DMA analysis of the recovery time after 3 cycles of compression at 30% strain*

402 Thermo-mechanical characterization

403 Finally, the thermo-mechanical properties of the foams were investigated using DMA. The figures S16
404 to S18 show the storage modulus E' and the loss factor $\tan\delta$ as a function of temperature for NIPTUs.
405 The transition from vitreous to elastic domain is associated to the α transition relaxation. The
406 temperature corresponding to the α transition (T_α) is associated to the glass transition temperature.
407 The value at the maximum of the $\tan\delta$ curves corresponds to the temperature T_α . The T_g determined
408 by DSC and the T_α follows the same tendency. The figures S16 to S18 show wide $\tan\delta$ peak for the
409 different foams, which shows a relative homogeneity of the foams despite the two different T_g
410 observed in DSC. Two T_α are expected in DMA, but it can be concluded the presence of the two
411 transitions in the wide transition observed in DMA. The different foams have similar T_α , which confirms
412 the same trend as the T_g measurement. All the T_α are comprised between 20 °C and 30 °C, which
413 confirms the trend, obtained by DSC.

414 4. Conclusion

415 Herein, we have described a cascade reaction strategy to obtain different structures of self-blown non-
416 isocyanate poly(thio-urethane) foams. The ring opening of the dithiocarbonate yields *in situ* thiol
417 moiety able to react with usual cyclic carbonate, which represents an interesting alternative to the
418 commercial PU foams. Our work demonstrated the synthesis of NIPU foams using the Pearson reaction
419 without the direct use of thiols in the formulation. This work used dithiocarbonate with a higher
420 reactivity than cyclic carbonate, which allowed to obtain a porous material at moderated temperature
421 (50°C). Moreover, we determined the required parameters in order to obtain a foam with a good
422 shape. A catalyst, 90°C and the ratio of DTC are crucial to obtain a well expanded NIPU foam by this
423 route. The properties of the foam can be modulated using different additives. The mechanical and
424 thermal properties obtained in this study is in adequation with the previous work carried out by Monie
425 *et al.* on the same foam structure.³³ The use of surfactant leads to microcellular material with low cell

426 interconnections. The use of additives using the Pickering stabilization led to bigger cells foams. Finally,
427 our investigation interestingly showed the absence of COS released during the curing of foams. The
428 thermal degradation could raise an issue but could be mitigated with flame retardant additives. To
429 conclude, this study shows the ability to obtain a NIPU foam with an internal bowing agent, at
430 moderate temperature, which corresponds to most of the applications of PUs. We can imagine mixing
431 carbon dioxide and carbon disulfide in order to have a mixture of cyclic carbonate on the same
432 molecule. Such process might avoid formulation step after the synthesis.

433 5. Acknowledgements

434 The authors would like to acknowledge Frédéric Fernandez from the MEA platform, Université de
435 Montpellier, for the SEM experiments and sample preparation. We would like to thank the financial
436 support provided by the NIPU-EJD project; this project has received funding from the European Union's
437 Horizon 2020 research and innovation programme under the Marie Skłodowska-Curie grant
438 agreement No 955700.

439

440 6. Appendix A. Supplementary material

441 Supplementary data are associated with this article.

442

443 7. References

444

- 445 (1) Bayer, O. Das Di-Isocyanat-Polyadditionsverfahren (Polyurethane). *Angew. Chemie A* **1947**, *59*
446 (9), 257–288.
- 447 (2) Randall, D.; Lee, S. *The Polyurethanes Book*; Randall, D., Lee, S., Eds.; J. Wiley, 2002.
- 448 (3) Wirpsza, Z. *Polyurethanes: Chemistry, Technology, and Applications*; Kemp, T. J., Ed.; E.
449 Horwood, 1993.
- 450 (4) Wendels, S.; Avérous, L. Biobased Polyurethanes for Biomedical Applications. *Bioact. Mater.*
451 **2021**, *6* (4), 1083–1106. <https://doi.org/10.1016/j.bioactmat.2020.10.002>.
- 452 (5) Singh, I.; Samal, S. K.; Mohanty, S.; Nayak, S. K. Recent Advancement in Plant Oil Derived Polyol-
453 Based Polyurethane Foam for Future Perspective: A Review. *Eur. J. Lipid Sci. Technol.* **2020**, *122*
454 (3), 1–23. <https://doi.org/10.1002/ejlt.201900225>.
- 455 (6) Akindoyo, J. O.; Beg, M. D. H.; Ghazali, S.; Islam, M. R.; Jeyaratnam, N.; Yuvaraj, A. R.
456 Polyurethane Types, Synthesis and Applications-a Review. *RSC Adv.* **2016**, *6* (115), 114453–
457 114482. <https://doi.org/10.1039/c6ra14525f>.
- 458 (7) Polyurethane, N.; Delebecq, E.; Pascault, J.; Boutevin, B.; Lyon, U. De. On the Versatility of
459 Urethane / Urea Bonds : Reversibility , Blocked. **2013**.
- 460 (8) Bello, D.; Herrick, C. A.; Smith, T. J.; Woskie, S. R.; Streicher, R. P.; Cullen, M. R.; Liu, Y.; Redlich,
461 C. A. Skin Exposure to Isocyanates: Reasons for Concern. *Environ. Health Perspect.* **2007**, *115*
462 (3), 328–335. <https://doi.org/10.1289/ehp.9557>.
- 463 (9) Stefanie Merenyi. *REACH: Regulation (EC) No 1907/2006: Consolidated Version (June 2012) with*
464 *an Introduction and Future Prospects Regarding the Area of Chemicals Legislation*; 2012.
- 465 (10) Gomez-Lopez, A.; Panchireddy, S.; Grignard, B.; Calvo, I.; Jerome, C.; Detrembleur, C.; Sardon,

- 466 H. Poly(Hydroxyurethane) Adhesives and Coatings: State-of-the-Art and Future Directions. *ACS*
 467 *Sustain. Chem. Eng.* **2021**, *9* (29), 9541–9562.
 468 <https://doi.org/10.1021/acssuschemeng.1c02558>.
- 469 (11) Maisonneuve, L.; Lamarzelle, O.; Rix, E.; Grau, E.; Cramail, H. Isocyanate-Free Routes to
 470 Polyurethanes and Poly(Hydroxy Urethane)S. *Chem. Rev.* **2015**, *115* (22), 12407–12439.
 471 <https://doi.org/10.1021/acs.chemrev.5b00355>.
- 472 (12) Wang, G.; Lopez, L.; Coile, M.; Chen, Y.; Torkelson, J. M.; Broadbelt, L. J. Identification of Known
 473 and Novel Monomers for Poly(Hydroxyurethanes) from Biobased Materials. *Ind. Eng. Chem.*
 474 *Res.* **2021**, *60* (18), 6814–6825. <https://doi.org/10.1021/acs.iecr.0c06351>.
- 475 (13) Beniah, G.; Fortman, D. J.; Heath, W. H.; Dichtel, W. R.; Torkelson, J. M. Non-Isocyanate
 476 Polyurethane Thermoplastic Elastomer: Amide-Based Chain Extender Yields Enhanced
 477 Nanophase Separation and Properties in Polyhydroxyurethane. *Macromolecules* **2017**, *50* (11),
 478 4425–4434. <https://doi.org/10.1021/acs.macromol.7b00765>.
- 479 (14) Unverferth, M.; Kreye, O.; Prohammer, A.; Meier, M. A. R. Renewable Non-Isocyanate Based
 480 Thermoplastic Polyurethanes via Polycondensation of Dimethyl Carbamate Monomers with
 481 Diols. *Macromol. Rapid Commun.* **2013**, *34* (19), 1569–1574.
 482 <https://doi.org/10.1002/marc.201300503>.
- 483 (15) Ecochard, Y.; Caillol, S. Hybrid Polyhydroxyurethanes: How to Overcome Limitations and Reach
 484 Cutting Edge Properties? *Eur. Polym. J.* **2020**, *137*, 109915.
 485 <https://doi.org/10.1016/j.eurpolymj.2020.109915>.
- 486 (16) Kihara, N.; Endo, T. Synthesis and Properties of Poly(Hydroxyurethane)S. *J. Polym. Sci. Part A*
 487 *Polym. Chem.* **1993**, *31*, 2765–2773.
- 488 (17) Carré, C.; Ecochard, Y.; Caillol, S.; Avérous, L. From the Synthesis of Biobased Cyclic Carbonate
 489 to Polyhydroxyurethanes: A Promising Route towards Renewable Non-Isocyanate
 490 Polyurethanes. *ChemSusChem* **2019**, *12* (15), 3410–3430.
 491 <https://doi.org/10.1002/cssc.201900737>.
- 492 (18) Poussard, L.; Mariage, J.; Grignard, B.; Detrembleur, C.; Jérôme, C.; Calberg, C.; Heinrichs, B.;
 493 De Winter, J.; Gerbaux, P.; Raquez, J. M.; Bonnaud, L.; Dubois, P. Non-Isocyanate Polyurethanes
 494 from Carbonated Soybean Oil Using Monomeric or Oligomeric Diamines to Achieve Thermosets
 495 or Thermoplastics. *Macromolecules* **2016**, *49* (6), 2162–2171.
 496 <https://doi.org/10.1021/acs.macromol.5b02467>.
- 497 (19) Nishikubo, T.; Iizawa, T.; Iida, M.; Isobe, N. Convenient Syntheses of Cyclic Carbonates by New
 498 Reaction of Oxiranes with *B*-Butyrolactone. *Tetrahedron Lett.* **1986**, *27* (32), 3741–3744.
- 499 (20) Gennen, S.; Grignard, B.; Thomassin, J. M.; Gilbert, B.; Vertruyen, B.; Jerome, C.; Detrembleur,
 500 C. Polyhydroxyurethane Hydrogels: Synthesis and Characterizations. *Eur. Polym. J.* **2016**, *84*,
 501 849–862. <https://doi.org/10.1016/j.eurpolymj.2016.07.013>.
- 502 (21) Kathalewar, M. S.; Joshi, P. B.; Sabnis, A. S.; Malshe, V. C. Non-Isocyanate Polyurethanes: From
 503 Chemistry to Applications. *RSC Adv.* **2013**, *3* (13), 4110–4129.
 504 <https://doi.org/10.1039/c2ra21938g>.
- 505 (22) Carré, C.; Bonnet, L.; Avérous, L. Original Biobased Nonisocyanate Polyurethanes: Solvent- and
 506 Catalyst-Free Synthesis, Thermal Properties and Rheological Behaviour. *RSC Adv.* **2014**, *4* (96),
 507 54018–54025. <https://doi.org/10.1039/c4ra09794g>.
- 508 (23) Benyahya, S.; Boutevin, B.; Caillol, S.; Lapinte, V.; Habas, J. P. Optimization of the Synthesis of
 509 Polyhydroxyurethanes Using Dynamic Rheometry. *Polym. Int.* **2012**, *61* (6), 918–925.

- 510 <https://doi.org/10.1002/pi.4159>.
- 511 (24) Panchireddy, S.; Grignard, B.; Thomassin, J. M.; Jerome, C.; Detrembleur, C. Bio-Based
512 Poly(Hydroxyurethane) Glues for Metal Substrates. *Polym. Chem.* **2018**, *9* (19), 2650–2659.
513 <https://doi.org/10.1039/c8py00281a>.
- 514 (25) Figovsky, O.; Shapovalov, L.; Leykin, A.; Birukova, O.; Potashnikova, R. Recent Advances in the
515 Development of Non-Isocyanate Polyurethanes Based On. *PU Mag.* **2013**, *10*
516 (August/September), 2–9.
- 517 (26) Blattmann, H.; Lauth, M.; Mülhaupt, R. Flexible and Bio-Based Nonisocyanate Polyurethane
518 (NIPU) Foams. *Macromol. Mater. Eng.* **2016**, *301* (8), 944–952.
519 <https://doi.org/10.1002/mame.201600141>.
- 520 (27) Grignard, B.; Thomassin, J. M.; Gennen, S.; Poussard, L.; Bonnaud, L.; Raquez, J. M.; Dubois, P.;
521 Tran, M. P.; Park, C. B.; Jerome, C.; Detrembleur, C. CO₂-Blown Microcellular Non-Isocyanate
522 Polyurethane (NIPU) Foams: From Bio- and CO₂-Sourced Monomers to Potentially Thermal
523 Insulating Materials. *Green Chem.* **2016**, *18* (7), 2206–2215.
524 <https://doi.org/10.1039/c5gc02723c>.
- 525 (28) Cornille, A.; Dworakowska, S.; Bogdal, D.; Boutevin, B.; Caillol, S. A New Way of Creating Cellular
526 Polyurethane Materials: NIPU Foams. *Eur. Polym. J.* **2015**, *66*, 129–138.
527 <https://doi.org/10.1016/j.eurpolymj.2015.01.034>.
- 528 (29) Cornille, A.; Guillet, C.; Benyahya, S.; Negrell, C.; Boutevin, B.; Caillol, S. Room Temperature
529 Flexible Isocyanate-Free Polyurethane Foams. *Eur. Polym. J.* **2016**, *84*, 873–888.
530 <https://doi.org/10.1016/j.eurpolymj.2016.05.032>.
- 531 (30) Xi, X.; Pizzi, A.; Gerardin, C.; Du, G. Glucose-Biobased Non-Isocyanate Polyurethane Rigid
532 Foams. *J. Renew. Mater.* **2019**, *7* (3), 301–312. <https://doi.org/10.32604/jrm.2019.04174>.
- 533 (31) Clark, J. H.; Farmer, T. J.; Ingram, I. D. V.; Lie, Y.; North, M. Renewable Self-Blowing Non-
534 Isocyanate Polyurethane Foams from Lysine and Sorbitol. *European J. Org. Chem.* **2018**, *2018*
535 (31), 4265–4271. <https://doi.org/10.1002/ejoc.201800665>.
- 536 (32) Mazurek-Budzyńska, M. M.; Rokicki, G.; Drzewicz, M.; Guńka, P. A.; Zachara, J. Bis(Cyclic
537 Carbonate) Based on D-Mannitol, D-Sorbitol and Di(Trimethylolpropane) in the Synthesis of
538 Non-Isocyanate Poly(Carbonate-Urethane)S. *Eur. Polym. J.* **2016**, *84*, 799–811.
539 <https://doi.org/10.1016/j.eurpolymj.2016.04.021>.
- 540 (33) Coste, G.; Negrell, C.; Caillol, S. From Gas Release to Foam Synthesis, the Second Breath of
541 Blowing Agents. *Eur. Polym. J.* **2020**, *140* (July), 110029.
542 <https://doi.org/10.1016/j.eurpolymj.2020.110029>.
- 543 (34) Monie, F.; Grignard, B.; Thomassin, J. M.; Mereau, R.; Tassaing, T.; Jerome, C.; Detrembleur, C.
544 Chemo- and Regioselective Additions of Nucleophiles to Cyclic Carbonates for the Preparation
545 of Self-Blowing Non-Isocyanate Polyurethane Foams. *Angew. Chemie - Int. Ed.* **2020**, *59* (39),
546 17033–17041. <https://doi.org/10.1002/anie.202006267>.
- 547 (35) Cornille, A.; Blain, M.; Auvergne, R.; Andrioletti, B.; Boutevin, B.; Caillol, S. A Study of Cyclic
548 Carbonate Aminolysis at Room Temperature: Effect of Cyclic Carbonate Structures and Solvents
549 on Polyhydroxyurethane Synthesis. *Polym. Chem.* **2017**, *8* (3), 592–604.
550 <https://doi.org/10.1039/c6py01854h>.
- 551 (36) Kihara, N.; Endo, T. Synthesis and Properties of Poly(Hydroxyurethane)S. *J. Polym. Sci. Part A*
552 *Polym. Chem.* **1993**, *31* (11), 2765–2773. <https://doi.org/10.1002/pola.1993.080311113>.

- 553 (37) Tomita, H.; Sanda, F.; Endo, T. Model Reaction for the Synthesis of Polyhydroxyurethanes from
554 Cyclic Carbonates with Amines: Substituent Effect on the Reactivity and Selectivity of Ring-
555 Opening Direction in the Reaction of Five-Membered Cyclic Carbonates with Amine. *J. Polym.*
556 *Sci. Part A Polym. Chem.* **2001**, *39* (21), 3678–3685. <https://doi.org/10.1002/pola.10009>.
- 557 (38) Tomita, H.; Sanda, F.; Endo, T. Polyaddition Behavior of Bis(Five- and Six-Membered Cyclic
558 Carbonate)s with Diamine. *J. Polym. Sci. Part A Polym. Chem.* **2001**, *39*, 860–867.
- 559 (39) Maisonneuve, L.; Wirotius, A. L.; Alfos, C.; Grau, E.; Cramail, H. Fatty Acid-Based (Bis) 6-
560 Membered Cyclic Carbonates as Efficient Isocyanate Free Poly(Hydroxyurethane) Precursors.
561 *Polym. Chem.* **2014**, *5* (21), 6142–6147. <https://doi.org/10.1039/c4py00922c>.
- 562 (40) Deng, L.; Sun, W.; Shi, Z.; Qian, W.; Su, Q.; Dong, L.; He, H.; Li, Z.; Cheng, W. Highly Synergistic
563 Effect of Ionic Liquids and Zn-Based Catalysts for Synthesis of Cyclic Carbonates from Urea and
564 Diols. *J. Mol. Liq.* **2020**, *316*, 113883. <https://doi.org/10.1016/j.molliq.2020.113883>.
- 565 (41) Pyo, S. H.; Hatti-Kaul, R. Selective, Green Synthesis of Six-Membered Cyclic Carbonates by
566 Lipase-Catalyzed Chemospecific Transesterification of Diols with Dimethyl Carbonate. *Adv.*
567 *Synth. Catal.* **2012**, *354* (5), 797–802. <https://doi.org/10.1002/adsc.201100822>.
- 568 (42) Gregory, G. L.; Ulmann, M.; Buchard, A. Synthesis of 6-Membered Cyclic Carbonates from 1,3-
569 Diols and Low CO₂ Pressure: A Novel Mild Strategy to Replace Phosgene Reagents. *RSC Adv.*
570 **2015**, *5* (49), 39404–39408. <https://doi.org/10.1039/c5ra07290e>.
- 571 (43) Lambeth, R. H.; Henderson, T. J. Organocatalytic Synthesis of (Poly)Hydroxyurethanes from
572 Cyclic Carbonates and Amines. *Polymer (Guildf)*. **2013**, *54* (21), 5568–5573.
573 <https://doi.org/10.1016/j.polymer.2013.08.053>.
- 574 (44) Blain, M.; Jean-Gérard, L.; Auvergne, R.; Benazet, D.; Caillol, S.; Andrioletti, B. Rational
575 Investigations in the Ring Opening of Cyclic Carbonates by Amines. *Green Chem.* **2014**, *16* (9),
576 4286–4291. <https://doi.org/10.1039/c4gc01032a>.
- 577 (45) Bourguignon, M.; Thomassin, J.; Grignard, B.; Vertruyen, B.; Detrembleur, C. Water - Borne
578 Isocyanate - Free Polyurethane Hydrogels with Adaptable Functionality and Behavior.
579 *Macromol. Rapid Commun.* **2021**, *42* (3), 2000482. <https://doi.org/10.1002/marc.202000482>.
- 580 (46) Henn, K. A.; Forsman, N.; Zou, T.; Österberg, M. Colloidal Lignin Particles and Epoxies for Bio-
581 Based, Durable, and Multiresistant Nanostructured Coatings. *ACS Appl. Mater. Interfaces* **2021**,
582 *13* (29), 34793–34806. <https://doi.org/10.1021/acscami.1c06087>.
- 583 (47) Bourguignon, M.; Thomassin, J. M.; Grignard, B.; Jerome, C.; Detrembleur, C. Fast and Facile
584 One-Pot One-Step Preparation of Nonisocyanate Polyurethane Hydrogels in Water at Room
585 Temperature. *ACS Sustain. Chem. Eng.* **2019**, *7* (14), 12601–12610.
586 <https://doi.org/10.1021/acssuschemeng.9b02624>.
- 587 (48) Kihara, N.; Nakawaki, Y.; Endo, T. Preparation of 1,3-Oxathiolane-2-Thiones by the Reaction of
588 Oxirane and Carbon Disulfide. *J. Org. Chem.* **1995**, *60* (2), 473–475.
589 <https://doi.org/10.1021/jo00107a034>.
- 590 (49) Motokucho, S.; Itagaki, Y.; Sudo, A.; Endo, T. Synthesis of a Novel Cyclic 5-Membered
591 Dithiocarbonate (DTC) Having Hydroxy Group and Its Application to Terminal Functionalization
592 of Polyurethane. *J. Polym. Sci. Part A Polym. Chem.* **2005**, *43* (16), 3711–3717.
593 <https://doi.org/10.1002/pola.20872>.
- 594 (50) Vanbiervliet, E.; Fouquay, S.; Michaud, G.; Simon, F.; Carpentier, J. F.; Guillaume, S. M. Non-
595 Isocyanate Polythiourethanes (NIPTUs) from Cyclodithiocarbonate Telechelic Polyethers.

- 596 *Macromolecules* **2019**, 52 (15), 5838–5849. <https://doi.org/10.1021/acs.macromol.9b00695>.
- 597 (51) Xu, C. R.; Zhang, Z.; Pan, C. Y.; Hong, C. Y. A Strategy Combining Quantitative Reactions and
598 Reversible-Covalent Chemistry for Sequential Synthesis of Sequence-Controlled Polymers with
599 Different Sequences. *Polymer (Guildf)*. **2019**, 172, 294–304.
600 <https://doi.org/10.1016/j.polymer.2019.04.017>.
- 601 (52) Besse, V.; Foyer, G.; Auvergne, R.; Caillol, S.; Boutevin, B. Access to Nonisocyanate
602 Poly(Thio)Urethanes: A Comparative Study. *J. Polym. Sci. Part A Polym. Chem.* **2013**, 51 (15),
603 3284–3296. <https://doi.org/10.1002/pola.26722>.
- 604 (53) Peyrton, J.; Avérous, L. Structure-Properties Relationships of Cellular Materials from Biobased
605 Polyurethane Foams. *Mater. Sci. Eng. R Reports* **2021**, 145 (March).
606 <https://doi.org/10.1016/j.mser.2021.100608>.
- 607 (54) Blain, M.; Cornille, A.; Boutevin, B.; Auvergne, R.; Benazet, D.; Andrioletti, B.; Caillol, S.
608 Hydrogen Bonds Prevent Obtaining High Molar Mass PHUs. *J. Appl. Polym. Sci.* **2017**, No. 44958,
609 1–13. <https://doi.org/10.1002/app.45646>.
- 610 (55) Dolci, E.; Michaud, G.; Simon, F.; Boutevin, B.; Fouquay, S.; Caillol, S. Remendable
611 Thermosetting Polymers for Isocyanate-Free Adhesives: A Preliminary Study. *Polym. Chem.*
612 **2015**, 6 (45), 7851–7861. <https://doi.org/10.1039/c5py01213a>.
- 613 (56) Peyrton, J.; Avérous, L. Structure-Properties Relationships of Cellular Materials from Biobased
614 Polyurethane Foams. *Mater. Sci. Eng. R Reports* **2021**, 145 (February).
615 <https://doi.org/10.1016/j.mser.2021.100608>.
- 616 (57) Tomita, H.; Sanda, F.; Endo, T. Polyaddition of Bis(Cyclic Thiocarbonate) with Diamines. Novel
617 Efficient Synthetic Method of Polyhydroxythiourethanes. *Macromolecules* **2001**, 34 (4), 727–
618 733. <https://doi.org/10.1021/ma001353l>.
- 619 (58) Cornille, A.; Dworakowska, S.; Bogdal, D.; Boutevin, B.; Caillol, S. A New Way of Creating Cellular
620 Polyurethane Materials: NIPU Foams. *Eur. Polym. J.* **2015**, 66, 129–138.
621 <https://doi.org/10.1016/j.eurpolymj.2015.01.034>.
- 622 (59) Yang, Z.; Peng, H.; Wang, W.; Liu, T. Crystallization Behavior of Poly(ϵ -Caprolactone)/Layered
623 Double Hydroxide Nanocomposites. *J. Appl. Polym. Sci.* **2010**, 116 (5), 2658–2667.
624 <https://doi.org/10.1002/app>.
- 625 (60) Speitel, L.; Walters, R. N.; Lyon, R. E. *Polymer Combustion Products at Constant Fuel/Oxygen*
626 *Ratios*; 2018.
- 627
- 628